

Cite this: *J. Mater. Chem. A*, 2015, 3, 24016

A multifunctional Eu MOF as a fluorescent pH sensor and exhibiting highly solvent-dependent adsorption and degradation of rhodamine B[†]

Qingguo Meng,[‡] Xuilian Xin,[‡] Liangliang Zhang,^a Fangna Dai,^a Rongming Wang^a and Daofeng Sun^{*a}

Due to their tunable structure and porosity, metal–organic frameworks have provided a new platform for fluorescence sensing and adsorption/separation of gas or organic molecules. Many studies have focused on sensing metal ions, anions, or organic molecules through fluorescence quenching or enhancement of MOFs, but studies on pH-fluorescence sensors are seldom reported. Furthermore, highly solvent-dependent adsorption and degradation of dye molecules based on functional MOFs has not been explored to date. In this study, we describe a multifunctional Eu MOF, [H₂O][Eu₃(HBPTC)₂(BPTC)(H₂O)₂]·4DMA (**UPC-5**, UPC = China University of Petroleum [East China]) based on a tetracarboxylate ligand. The luminescence intensity of **UPC-5** is strongly correlated with the pH value in the pH range from 7.5 to 10.0, and a linear relationship between pH value and fluorescent intensity is observed. Another attractive property of **UPC-5** is that its Li-exchanged form, Li-**UPC-5**, possesses solvent-dependent adsorption and degradation of rhodamine B. The highly efficient degradation or decolorization of rhodamine B with long-term stability and activity gives Li-**UPC-5** a potential advantage in treating rhodamine B pollution.

Received 4th July 2015
Accepted 21st October 2015

DOI: 10.1039/c5ta04989j

www.rsc.org/MaterialsA

Introduction

Recently, luminescent materials based on metal–organic frameworks (MOFs) or coordination polymers have been of extensive interest due to their wide range of potential applications in optics, displays, luminescence-based sensors, light-emitting devices (LEDs) or proofs for clinical use.^{1–7} In particular, luminescent porous MOF-based sensors have developed rapidly and their applications in simply detecting metal ions,^{8–10} anions,^{11,12} small organic molecules,^{13,14} explosive and explosive-like molecules^{15,16} have been widely documented. However, pH-dependent fluorescent sensors based on porous MOFs have seldom been reported. To design and synthesize such a fluorescent MOF-based sensor, the framework should contain a certain functional group or unit that can accept a proton or OH[−] group in a certain pH range without causing the collapse of the framework. Very recently, Zhou *et al.* reported an

exceptionally stable, porphyrinic Zr metal–organic framework (PCN-225) exhibiting pH-dependent fluorescence.¹⁷ The PCN-225 MOF can remain intact in aqueous solutions at pHs ranging from 1 to 11; furthermore, the fluorescence intensity of PCN-225 is strongly correlated with the pH value of the dispersed solution in the experimental pH range from 0 to 10.2, which derives from the pyridine-type nitrogen atoms in the porphyrin center being able to accept a proton to destroy the π -electron conjugated double-bond system of porphyrin.

The tunable structures and porosities of MOFs have provided a platform for the applications in adsorption/separation of gas or organic molecules. Generally, the separation of gas/organic molecules is highly dependent on the host–guest interaction between the framework and the gas/organic molecules. Dye molecules, as widely used chemicals in many industries,¹⁸ have caused environmental pollution due to their poor biodegradability.¹⁹ Thus, the selective removal/enrichment or degradation of dye molecules is very important for environmental protection. In the past several years, the adsorption or separation of dye molecules by porous MOFs has been reported in the literature.^{20–22} On the basis of current research, there are two ways for the separation of dye molecules by porous MOFs: size-exclusion effect and ionic selectivity. The former was fully illustrated by Xu's group through the effective separation of large dye molecules by Zn/Cd MOFs with large channels.^{23,24} The separation of dye molecules through ionic selectivity was also reported recently.²⁵ Although semiconductor-mediated or metal

^aState Key Laboratory of Heavy Oil Processing, China University of Petroleum (East China), College of Science, Qingdao, Shandong 266580, People's Republic of China. E-mail: dfsun@upc.edu.cn

^bChemistry & Chemical and Environmental Engineering College, Weifang University, Weifang, Shandong 261061, People's Republic of China

[†] Electronic supplementary information (ESI) available: TGA, PXRD, gas adsorption isotherms and the solid-state luminescent emission spectra and additional figures for **UPC-5**. CCDC 1023321. For ESI and crystallographic data in CIF or other electronic format see DOI: 10.1039/c5ta04989j

[‡] These two authors contributed equally to this work.

oxides-based photodegradation of dye pollutants under visible-light irradiation has been documented,^{26–28} reports on highly selective adsorption^{23–25} and efficient degradation of dye molecules by MOFs are still rare.²⁹ Furthermore, highly solvent-dependent selectivity and degradation to dye molecules based on a multifunctional MOF has not been explored so far. In this contribution, we report a multifunctional Eu MOF, $[\text{H}_3\text{O}][\text{Eu}_3(\text{HBPTC})_2(\text{BPTC})(\text{H}_2\text{O})_2] \cdot 4\text{DMA}$ (**UPC-5**, UPC = China University of Petroleum [East China]) (H_4BPTC = 3,3',5,5'-biphenyltetracarboxylate), which possesses pH-dependent fluorescence in the pH range of 7–10, and highly solvent-dependent adsorption and degradation of rhodamine B based on ionic selectivity.

Results and discussion

1. Crystal structure of UPC-5

Colorless crystals of **UPC-5** were obtained by solvothermal reaction of H_4BPTC and $\text{Eu}(\text{NO}_3)_3 \cdot 6\text{H}_2\text{O}$ in $\text{DMA}/\text{H}_2\text{O}$ at 90 °C for 2 days. The resultant crystalline sample of **UPC-5** was not soluble in common solvents such as acetone, DMF or DMSO. The crystal structure was determined by single-crystal X-ray diffraction, and the formula of $[\text{H}_3\text{O}][\text{Eu}_3(\text{HBPTC})_2(\text{BPTC})(\text{H}_2\text{O})_2] \cdot 4\text{DMA}$ was further confirmed by thermogravimetric analysis and elemental analysis.

UPC-5 crystallizes in triclinic space group $P\bar{1}$, and the asymmetric unit consists of one and a half Eu ions, one and a half BPTC ligands and one coordinated water molecule. As shown in Fig. 1, there are two types of BPTC ligands (^aBPTC, ^bBPTC) with different coordination modes: ^aBPTC bridges six Eu ions, and one of carboxylate group is protonated, and ^bBPTC also links six Eu ions but all the carboxylate groups are deprotonated. Meanwhile, two types of Eu ions (Eu1, Eu2) with different coordination numbers exist in **UPC-5**: Eu1 is coordinated by eight oxygen atoms from six carboxylate groups, and

Eu2 is coordinated by nine oxygen atoms from eight carboxylate groups and one coordinated water molecule. Thus, one Eu1 and two Eu2 ions are connected by six carboxylate groups from different ligands to form a trinuclear SBU, which is similar to another transition metal “hourglass” SBU.³⁰ The trinuclear SBUs are first linked by ^aBPTC ligands in the *ab* plane to generate a 2D layer, which is further connected by ^bBPTC ligands along *c* axis to give rise to a 3D open anionic framework with 1D channels along *b* axis. The dimensions of the channels are about 10.0 × 15.0 Å, and the protonated H_2O molecules reside in the channels to balance the charge of the whole framework. The solvent-accessible volume calculated by PLATON³¹ is 664.5 Å³, corresponding to 41.1% of unit cell of **UPC-5**.

It should be pointed out that there exists a 1D supramolecular chain generated through the link of strong hydrogen bonds among the mono-protonated ^aBPTC ligands, as shown in Fig. 1d. The distance between the O···O is about 2.513 Å with the O···H···O angle of 169.10°, indicating a strong hydrogen bonding interaction. On the basis of the crystal data, the H atom does not belong to any O atom, since the two O···H bonds are 1.357 and 1.167 Å, which may illustrate that the two O atoms are sharing the same H atom. The hydrogen bond distance presented here is also in the range in which the electron-transfer or hydrogen-bonded proton-transfer can occur between the two O atoms.^{32,33}

2. Gas-uptake property

Considering the existence of 1D channels, gas-uptake measurements for desolvated **UPC-5** were carried out. Before the measurement, the as-synthesized crystal sample of **UPC-5** was immersed in methanol to exchange the uncoordinated DMA and water molecules. The exchanged sample was activated at 60 °C under vacuum for 10 hours. As shown in Fig. 2, **UPC-5** exhibits a typical type-I adsorption isotherm for N_2 at 77 K, with a surface area of 432 m² g⁻¹. After the exchange of H_3O^+ by Li^+ in the channels (according to the ICP results, about 83% H^+ was exchanged by Li^+ after being immersed in fresh LiCl methanol solution for 12 hours), the surface area of the resultant **Li-UPC-5** increases slightly to 443.7 m² g⁻¹. These results indicate that

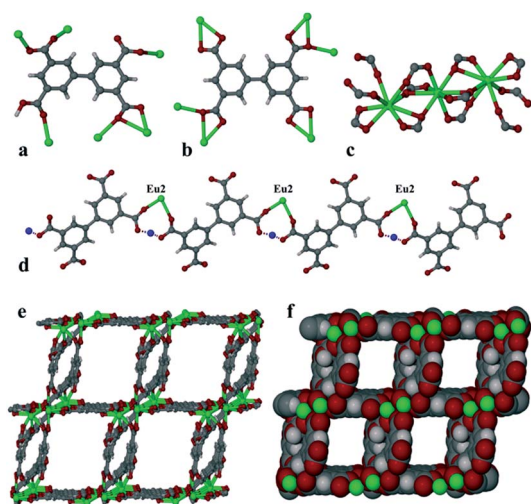


Fig. 1 The coordination modes of ^aBPTC (a), ^bBPTC (b); the trinuclear “hourglass” SBU (c); the 1D supramolecular chain (d); the 3D porous framework with 1D channel along the *b* axis (e); and space-filling representation of the 3D porous framework (f). The uncoordinated solvent molecules are omitted for clarity.

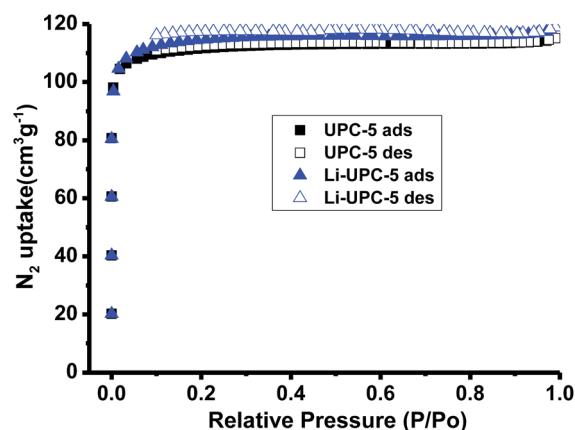


Fig. 2 N_2 adsorption isotherms for **UPC-5** and **Li-UPC-5**.

UPC-5 and Li-UPC-5 can sustain their frameworks after the removal of the solvates in the channels. The gas uptakes for H₂ and CO₂ were also measured, and are shown in Fig. S4–S11.†

3. Fluorescent pH sensor

The luminescence measurement reveals that, upon excitation at 331 nm, UPC-5 exhibits luminescence at $\lambda_{\text{max}} = 593, 617, 653, 696$ nm, among which the emissions at 653 and 696 nm are very weak, as shown in Fig. S12.† The emissions of UPC-5 show the characteristic transitions of the Eu³⁺ ion and can probably be assigned to ⁵D₀ → ⁷F₁, ⁵D₀ → ⁷F₂, ⁵D₀ → ⁷F₃, and ⁵D₀ → ⁷F₄ transitions, respectively. Due to the existence of protonated carboxylate in UPC-5, it can react with an OH[−] group to be deprotonated, which may cause the change of the luminescence. Thus, pH-dependent fluorescence measurement was carried out. The crystalline sample of UPC-5 was ground and dispersed in water solution. As shown in Fig. S13 and S14,† the photoluminescence intensity of UPC-5 decreases gradually with time after adding 1d NaOH solution. When the pH value increases from 7 to 7.5, the luminescent intensity of UPC-5 increases sharply to reach the maximum (Fig. 3), which may derive from the introduction of the Na⁺ ion into the channels highly influencing the luminescence emission of Eu³⁺ ions. However, when the pH value increases from 7.5 to 10, the intensity of the luminescence gradually decreases. Interestingly, the luminescence intensity of UPC-5 is strongly correlated with the pH value in this pH range from 7.5 to 10.0, and a linear relationship between pH value and fluorescent intensity is observed. The reason for this may be that at lower basicity, the OH[−] groups react with the proton in ^oBPTC ligands and destroy the electron transfer and the conjugate system, gradually influencing the characteristic transitions of the Eu³⁺ ion (quenching effect), as found in the porphyrin system.³⁴ In comparison, when the pH is higher than 10, the emission intensity decreases significantly, which may result from the deprotonation of the carboxylate group significantly destroying the conjugated system and the electron transfer. As is known, it

is very important for health to keep blood and other body fluids alkaline. When the body keeps a pH value of 7.4, it has the best power of spontaneous healing. UPC-5 possesses the highest emission intensity at pH 7.5, and has a linear relationship between pH value and fluorescent intensity in the pH range from 7.5 to 10.0, which may suggest that UPC-5 can act as pH-dependent fluorescent sensor.³⁵

4. Solvent-dependent adsorption of rhodamine B

Another attractive property of porous MOFs is the separation or enrichment of organic molecules, including dye molecules. Due to the existence of the H₃O⁺ cation in the channels, the adsorption or separation of dye molecules based on ionic selectivity for UPC-5 was carried out. Dye molecules with different sizes and charges were selected for the test. To our surprise, UPC-5 possesses highly solvent-dependent selectivity for rhodamine B, but there is no adsorption of other dye molecules. We found that when the as-synthesized crystals of UPC-5 were soaked in methanol solution containing LiCl to exchange H₃O⁺ with Li⁺, the resultant Li-UPC-5 sample possesses faster adsorption to rhodamine B, as shown in Fig. S15 and S16.† Thus, the following experiments on adsorption and degradation are based on Li-UPC-5.

When the crystals of Li-UPC-5 were soaked in an acetone solution of rhodamine B, the colorless crystals gradually became colored (pink) in three hours and the color of the solution changed from pink to colorless, indicating that rhodamine B could be efficiently adsorbed by crystals of Li-UPC-5 (Fig. 4a). As a comparison, when the crystals of Li-UPC-5 were soaked in acetone solution of methyl violet or other anionic dye molecules, there was almost no adsorption even after 12 hours, indicating that Li-UPC-5 can selectively adsorb rhodamine B (Fig. 4b and c). The capability of Li-UPC-5 to adsorb rhodamine B from acetone solution was evaluated through UV/Vis

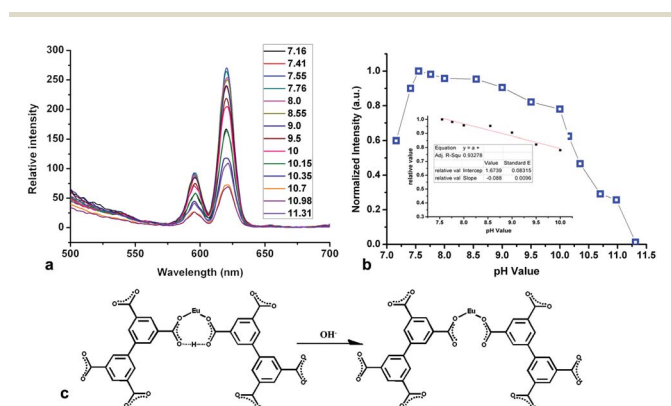


Fig. 3 (a) pH dependent fluorescence of UPC-5 in aqueous solution with pH ranging from 7 to 11. (b) Blue squares show the fluorescence emission at 617 nm at different pH values. Inset: the linear relationship between pH value and fluorescent intensity in the pH range from 7.5 to 10.0. (c) Schematic deprotonation process of carboxylate group under basic media.

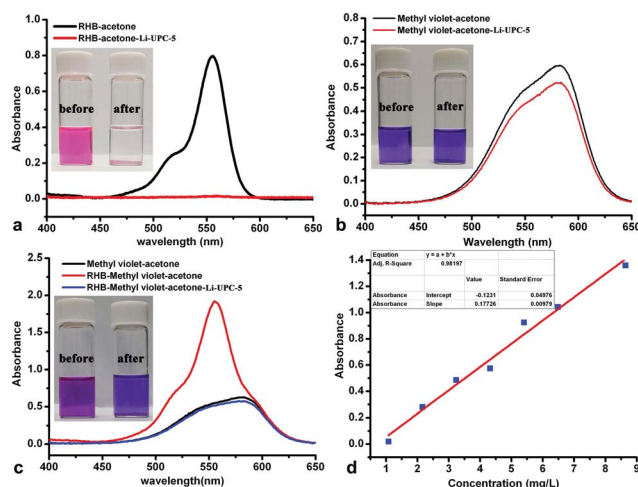


Fig. 4 UV-vis spectra of RHB in acetone (a), methyl violet in acetone (b), mixed dyes of RHB and methyl violet in acetone (c) before and after the addition of Li-UPC-5. The inset photographs highlight the adsorption effects showing before (left) and after (right) adsorption. (d) Standard curve for rhodamine B concentration.

spectroscopy. According to the standard curve for rhodamine B concentration (Fig. 4d), the adsorptivity of Li-UPC-5 is 4.38 mg g^{-1} , which is slightly bigger than other MOFs.²⁵ The adsorption of rhodamine B into the channels of Li-UPC-5 can be further confirmed by gas uptake measurement. By fitting the N_2 isotherm, the Brunauer–Emmett–Teller (BET) surface area of the active Li-UPC-5 is $443.7 \text{ m}^2 \text{ g}^{-1}$. After the adsorption of rhodamine B, there is almost no adsorption of N_2 molecules, indicating that rhodamine B molecules were adsorbed into the pores of Li-UPC-5 (Fig. 5).

More interestingly, the adsorption capacity of rhodamine B by Li-UPC-5 is highly determined by the solvent. The polarity of acetone is about 5.4 and the ability for acetone to form hydrogen bonds with other organic molecules is somewhat weak, compared to H_2O , DMF, MeOH *etc.* The adsorption measurements for rhodamine B in H_2O and MeOH reveal that there are almost no adsorptions in these solvents even after several days, as detected by UV/Vis spectroscopy (Fig. 6). Because the polarity of H_2O and MeOH is much stronger than acetone, in order to understand the effect of the solvents on the adsorption capacity of rhodamine B, two solvents with similar polarity, isopropanol and chloroform, were used. As shown in Fig. 6c, there is almost no adsorption of rhodamine B in isopropanol solution, as detected by UV/Vis spectroscopy; however, Li-UPC-5 can efficiently adsorb rhodamine B in chloroform solution, although the adsorption capacity is lower than that in acetone solution. These results indicate that if the solvent can act as the donor or acceptor of hydrogen bond (protic solvent) to form hydrogen-bonding interactions with rhodamine B, then the adsorption capacity in these solvents is very low. On the contrary, Li-UPC-5 can efficiently adsorb rhodamine B in the solvents that possess low ability to form hydrogen bonds (aprotic solvent). Hence, the adsorption of rhodamine B in aprotic solvent is much higher than that in protic solvent, and the higher the polarity of the aprotic solvent, the larger the adsorption capacity.

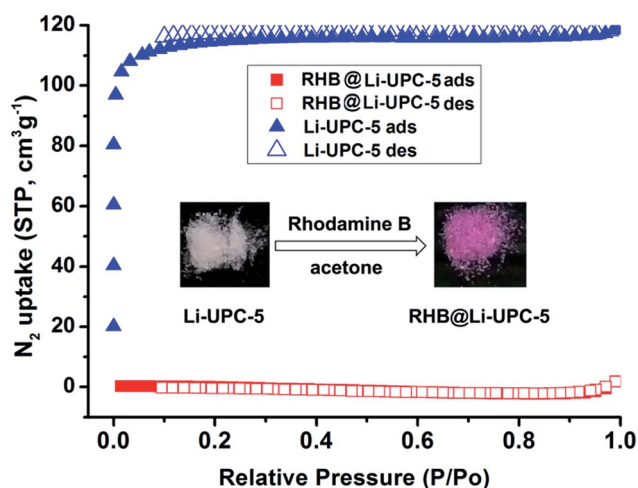


Fig. 5 N_2 adsorption isotherm before and after adsorption of rhodamine B. Inset: the crystal colors of Li-UPC-5 and RHB@Li-UPC-5.

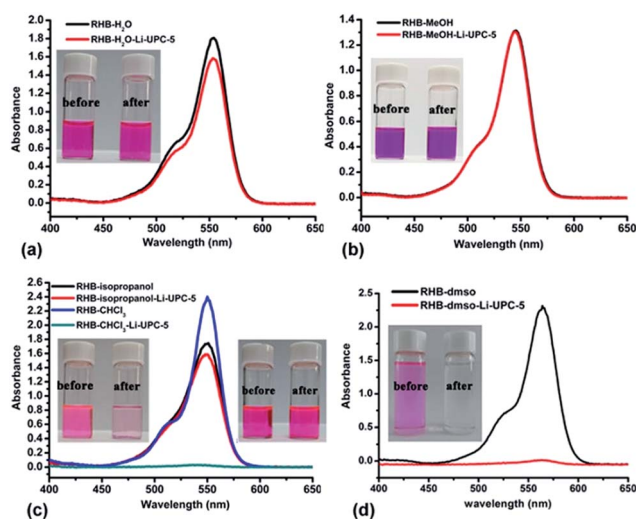


Fig. 6 UV-vis spectra of RHB in H_2O (a), MeOH (b), isopropanol and CH_2Cl_2 (c), and DMSO (d) before and after the addition of Li-UPC-5. The inset photographs highlight the adsorption effects showing before (left) and after (right) adsorption.

5. Degradation of rhodamine B in DMSO solution

To further confirm the phenomenon mentioned above, another aprotic solvent with higher polarity, dimethyl sulfoxide (DMSO), was used to test the adsorption capacity of Li-UPC-5. To our surprise, Li-UPC-5 can efficiently degrade rhodamine B in DMSO solution under natural light. As shown in Fig. 6d, the color of the solution changed from pink to colorless in several minutes, whereas the colorless crystals remain unchanged. Furthermore, the UV/Vis spectroscopy measurements on the solution and the solid reveal that the characteristic adsorption peaks at 355 and 565 nm for rhodamine B disappeared (Fig. S17[†]), indicating that rhodamine B, at least the chromophore, was degraded. The degradation of rhodamine B by Li-UPC-5 is fast and highly efficient, and it can be completely degraded after 15 minutes, as detected by UV/Vis spectroscopy. A control experiment with $\text{Eu}(\text{NO}_3)_3 \cdot 6\text{H}_2\text{O}$ and H_4BPTC was also carried out: no degradation was observed with $\text{Eu}(\text{NO}_3)_3 \cdot 6\text{H}_2\text{O}$ and H_4BPTC as the catalyst, indicating that the degradation should occur in the pores of Li-UPC-5 after rhodamine B was adsorbed into the channels.

For the purpose of the practical applications, it is essential for the photocatalyst to possess long-term stability and activity. In the present case, after each run of the rhodamine B total decolorization, the solution was removed from the test tube, and the identical amount of rhodamine B in DMSO solution was then added into the test tube for another run reaction. Fig. 7 shows the results of rhodamine B decolorization during 20 consecutive cycles. Almost 100% decolorization of rhodamine B was achieved for each run reaction, and no obvious loss of the activity for rhodamine B decolorization was observed during 20 cycles, indicating that Li-UPC-5 possesses excellent long-term stability. The activity of Li-UPC-5 presented here is much higher than that of other MOF-based photocatalysts and Degussa P-25.^{36–38}

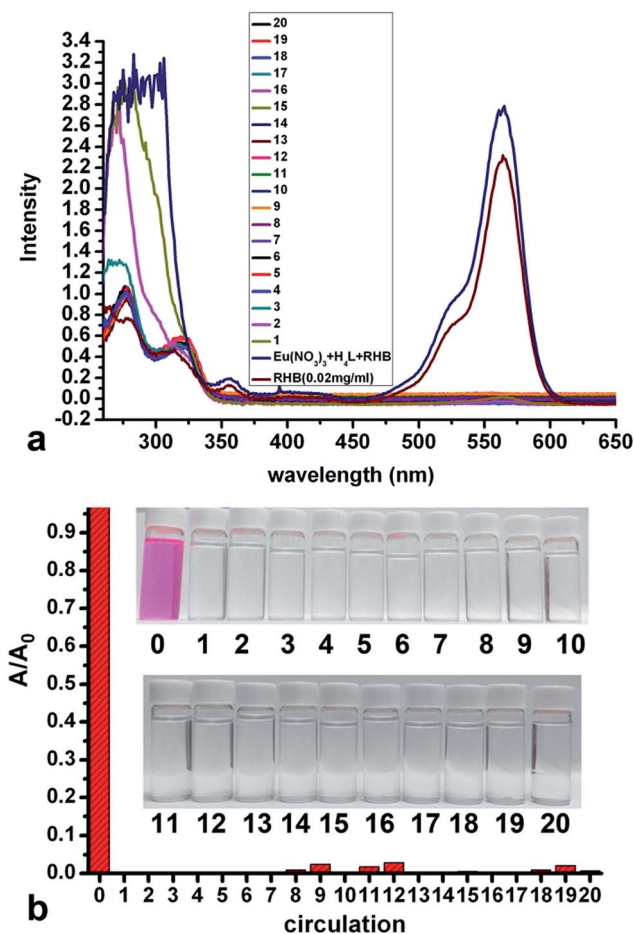


Fig. 7 (a) UV-vis spectra of RHB in DMSO (0.02 mg ml^{-1}), $(\text{Eu}(\text{NO}_3)_3 + \text{H}_4\text{BPTC} + \text{RHB})$ in DMSO, and after the degradation for 20 cycles. (b) The relative UV-vis intensity at 554 nm for the degradation of RHB in 20 cycles. Inset: the photographs highlight the degradation effects for 20 cycles.

To analyze the degradation product, proton NMR study was carried out (Fig. S18[†]). By comparison of the proton NMR spectra for before and after degradation of RHB, it revealed that the peaks at ~ 3.5 and ~ 1.0 ppm for the $-\text{CH}_2\text{CH}_3$ group disappear, while new peaks at ~ 13 ppm, which should be assigned to the proton of the carboxylate group, appear after the degradation. These results indicate the main products of the degradation should be phthalic acid and benzoic acid, as found in other literature.^{39,40}

Conclusions

In summary, a multifunctional europium-organic framework (UPC-5) based on a tetracarboxylate ligand was synthesized and characterized. The anionic porous framework and the existence of protonated carboxylate in UPC-5 make it possess multiple potential functionalities. The results and conclusions of these investigations are summarized as follows: (1) due to the existence of a protonated carboxylate group and a 1D supramolecular chain formed by sharing the proton, UPC-5 can be stable

under alkaline conditions, and shows a linear relationship between pH value and fluorescent intensity at the pH range from 7.5 to 10. This result makes UPC-5 possess potential application as a pH-dependent fluorescent sensor; (2) after the replacement of H_3O^+ by Li^+ , the Li^+ cations in the channels can efficiently exchange with cationic dye molecules, which endows Li-UPC-5 with highly selective adsorption of rhodamine B upon other ionic dye molecules in acetone solution. Furthermore, the adsorption of rhodamine B by Li-UPC-5 is highly determined by the solvent, and aprotic solvents are favorable for the adsorption of rhodamine B; (3) the most attractive property of this work is that Li-UPC-5 can efficiently degrade rhodamine B in DMSO solution under natural light. The degradation is fast and the catalyst possesses long-term stability and activity. Although the adsorption and degradation of rhodamine B in organic solvents may somewhat limit its practical application, the fast and efficient degradation of rhodamine B gives Li-UPC-5 an advantage in treating rhodamine B pollution at high concentrations. Deep study of the degradation mechanism is currently underway in our lab.

Experimental

Materials and measurements

Commercially available reagents were used as received without further purification. Elemental analyses (C, H, N) were performed with a Perkin Elmer 240 elemental analyzer. Thermal gravimetric analysis (TGA) was performed under N_2 on a Perkin Elmer TGA 7 instrument. Photoluminescence spectra were performed on a Perkin Elmer LS 50B luminescence spectrometer.

Synthesis of UPC-5

H_4BPTC (64 mg, 0.2 mmol) and $\text{Eu}(\text{NO}_3)_3 \cdot 6\text{H}_2\text{O}$ (223 mg, 0.5 mmol) were dissolved in 50 ml of $\text{DMA-H}_2\text{O}$ (1 : 1). The solution was split into 50 portions and placed in glass tubes, then 0.25 ml of HNO_3 (6 M) was added into each tube. The sealed tubes were slowly heated to 90°C from room temperature in 5 hours, then kept at 90°C for 2 days. After slowly cooled to 30°C in 13 hours, colorless block crystals of UPC-5 were separated in 49.5% yield based on H_4BPTC . EA (%) calculated for $[\text{H}_3\text{O}][\text{Eu}_3(\text{HBPTC})_2(\text{BPTC})(\text{H}_2\text{O})_2] \cdot 4\text{DMA}$: C, 41.78; H, 3.45; N, 3.04; found: C, 42.35; H, 3.58; N, 3.03.

Single-crystal X-ray diffraction study

Single-crystal X-ray diffraction was performed using an Agilent Xcalibur Eos Gemini diffractometer with enhance (Mo) X-ray source (Mo-K α , $\lambda = 0.71073 \text{ \AA}$). Contributions to scattering from all solvent molecules were removed using the SQUEEZE routine of PLATON; structures were then refined again using the data generated. Crystallographic data (excluding structure factors) for the structure reported in this paper have been deposited in the Cambridge Crystallographic Data Centre with CCDC Number: 1023321.[†] Full experimental details and crystallographic analysis are given in the ESI.[†]

Acknowledgements

This work was supported by the NSFC (Grant No. 21271117, 21571187), NCET-11-0309, the Shandong Natural Science Fund for Distinguished Young Scholars (JQ201003), Shandong Provincial Natural Science Foundation (ZR2015BM005) and the Fundamental Research Funds for the Central Universities (13CX05010A, 14CX02158A).

Notes and references

- L. Kreno, K. Leong, O. Farha, M. Allendorf, R. van Duyne and J. Hupp, *Chem. Rev.*, 2012, **112**, 1105–1125.
- Y. Cui, Y. Yue, G. Qian and B. Chen, *Chem. Rev.*, 2012, **112**, 1126–1162.
- M. D. Allendorf, C. A. Bauer, R. K. Bhakta and R. J. T. Houk, *Chem. Soc. Rev.*, 2009, **38**, 1330–1352 and references therein.
- Z. C. Hu, B. J. Deibert and J. Li, *Chem. Soc. Rev.*, 2014, **43**, 5815–5840.
- Y. Takashima, V. Martinez, S. Furukawa, M. Kondo, S. Shimomura, H. Uehara, M. Nakahama, K. Sugimoto and S. Kitagawa, *Nat. Commun.*, 2011, **2**, 168–175.
- C. Y. Sun, X. L. Wang, X. Zhang, C. Qin, P. Li, Z. M. Su, D. X. Zhu, G. G. Shan, K. Z. Shao, H. Wu and J. Li, *Nat. Commun.*, 2013, **4**, 2717–2724.
- D. F. Sava, L. E. Rohwer, M. A. Rodriguez and T. M. Nenoff, *J. Am. Chem. Soc.*, 2012, **134**, 3983–3986.
- J. He, M. Q. Zha, J. S. Cui, M. Zeller, A. D. Hunter, S. M. Yiu, S. T. Lee and Z. T. Xu, *J. Am. Chem. Soc.*, 2013, **135**, 7807–7810.
- B. L. Chen, L. B. Wang, Y. Q. Xiao, F. R. Fronczek, M. Xue, Y. J. Cui and G. D. Qian, *Angew. Chem., Int. Ed.*, 2009, **48**, 508–511.
- Y. W. Li, J. R. Li, L. F. Wang, B. Y. Zhou, Q. Chen and X. H. Bu, *J. Mater. Chem. A*, 2013, **1**, 495–499.
- J. M. Zhou, W. Shi, N. Xu and P. Cheng, *Inorg. Chem.*, 2013, **52**, 8082–8090.
- B. L. Chen, L. B. Wang, F. Zapata, G. D. Qian and E. B. Lobkovsky, *J. Am. Chem. Soc.*, 2008, **130**, 6718–6719.
- Z. M. Hao, X. Z. Song, M. Zhu, X. Meng, S. N. Zhao, S. Q. Su, W. T. Yang, S. Y. Song and H. J. Zhang, *J. Mater. Chem. A*, 2013, **1**, 11043–11050.
- Z. Z. Lu, R. Zhang, Y. Z. Li, Z. J. Guo and H. G. Zheng, *J. Am. Chem. Soc.*, 2011, **133**, 4172–4174.
- S. Pramanik, C. Zheng, X. Zhang, T. J. Emge and J. Li, *J. Am. Chem. Soc.*, 2011, **133**, 4153–4155.
- S. S. Nagarkar, B. Joarder, A. K. Chaudhari, S. Mukherjee and S. K. Ghosh, *Angew. Chem., Int. Ed.*, 2013, **52**, 2881–2885.
- H. L. Jiang, D. W. Feng, K. C. Wang, Z. Y. Gu, Z. W. Wei, Y. P. Chen and H.-C. Zhou, *J. Am. Chem. Soc.*, 2013, **135**, 13934–13938.
- B. Adhikari, G. Palui and A. Banerjee, *Soft Matter*, 2009, **5**, 3452–3460.
- M. A. Al-Ghouti, M. Khraisheh, S. J. Allen and M. N. Ahmad, *J. Environ. Manage.*, 2003, **69**, 229–238.
- R. Ameloot, F. Vermoortele, W. Vanhove, M. B. J. Roeffaers, B. F. Sels and D. E. de Vos, *Nat. Chem.*, 2011, **3**, 382–387.
- S. B. Han, Y. H. Wei, C. Valente, I. Lagzi, J. J. Gassensmith, A. Coskun, J. F. Stoddart and B. A. Grzybowski, *J. Am. Chem. Soc.*, 2010, **132**, 16358–16361.
- C. Zou, Z. J. Zhang, X. Xu, Q. H. Gong, J. Li and C. D. Wu, *J. Am. Chem. Soc.*, 2012, **134**, 87–90.
- Y. Q. Lan, H. L. Jiang, S. L. Li and Q. Xu, *Adv. Mater.*, 2011, **23**, 5015–5020.
- H. L. Jiang, Y. Tatsu, Z. H. Lu and Q. Xu, *J. Am. Chem. Soc.*, 2010, **132**, 5586–5587.
- C. Y. Sun, X. L. Wang, C. Qin, J. L. Jin, Z. M. Su, P. Huang and K. Z. Shao, *Chem.–Eur. J.*, 2013, **19**, 3639–3645.
- C. C. Chen, W. H. Ma and J. C. Zhao, *Chem. Soc. Rev.*, 2010, **39**, 4206–4219 and references therein.
- Z. H. Wang, W. H. Ma, C. C. Chen and J. C. Zhao, *J. Hazard. Mater.*, 2009, **168**, 1246–1252.
- Y. G. Zhou, J. L. Long, Q. Gu, H. X. Lin, H. Lin and X. X. Wang, *Inorg. Chem.*, 2012, **51**, 12594–12596.
- L. L. Wen, J. B. Zhao, K. L. Lv, Y. H. Wu, K. J. Deng, X. K. Leng and D. F. Li, *Cryst. Growth Des.*, 2012, **12**, 1603–1612.
- D. F. Sun, Y. X. Ke, D. J. Collins, G. A. Lorigan and H. C. Zhou, *Inorg. Chem.*, 2007, **46**, 2725–2734.
- A. L. Spek, *J. Appl. Crystallogr.*, 2003, **36**, 7–13.
- G. Xu, G. C. Guo, M. S. Wang, Z. J. Zhang, W. T. Chen and J. S. Huang, *Angew. Chem., Int. Ed.*, 2007, **46**, 3249–3251.
- A. Kobayashi, M. Dosen, M. Chang, K. Nakajima, S. Noro and M. Kato, *J. Am. Chem. Soc.*, 2010, **132**, 15286–15298.
- S. Thyagarajan, T. Leiding, S. P. Arskold, A. V. Cheprakov and S. A. Vinogradov, *Inorg. Chem.*, 2010, **49**, 9909–9920.
- D. G. Smith, B. K. McMahon, R. Pal and D. Parker, *Chem. Commun.*, 2012, **48**, 8520–8522.
- Z. T. Yu, Z. L. Liao, Y. S. Jiang, G. H. Li, G. D. Li and J. S. Chen, *Chem. Commun.*, 2004, 1814–1815.
- P. Mahata, G. Madras and S. Natarajan, *J. Phys. Chem. B*, 2006, **110**, 13759–13768.
- J. J. Du, Y. P. Yuan, J. X. Sun, F. M. Peng, X. Jiang, L. G. Qiu, A. J. Xie, Y. H. Shen and J. F. Zhu, *J. Hazard. Mater.*, 2011, **190**, 945–951.
- J. Li, W. Ma, P. Lei and J. Zhao, *J. Environ. Sci.*, 2007, **19**, 892–896.
- S. Gazi, R. Ananthakrishnan and N. D. P. Singh, *J. Hazard. Mater.*, 2010, **183**, 894–901.